

Induced Overvoltages on the SF₆ Substation Enclosure Caused by Switching

Preliminary communication

Stjepan Jonjić

Faculty of Electrical Engineering
J.J. Strossmayer University of Osijek, Croatia
sjonjic@etfos.hr

Zoran Baus

Faculty of Electrical Engineering
J.J. Strossmayer University of Osijek, Croatia
zoran.baus@tvz.hr

Marinko Barukčić

Faculty of Electrical Engineering
J.J. Strossmayer University of Osijek, Croatia
marinko.barukcic@etfos.hr

This work was presented on the scientific-professional symposium "Development of Power Engineering in Croatia" which was held on 21 October 2011 at the Faculty of Electrical Engineering in Osijek on the occasion of the 150th Anniversary of the Croatian Academy of Sciences and Arts.

Abstract – This paper investigates overvoltages on the SF₆ substation enclosure caused by the switching operation of the interrupter. The paper analyzes the amplitude and the overvoltage duration on the substation enclosure. Switching overvoltages take part in the everyday drive of HV substations and constitute an undesired phenomenon that may often, beside transient disturbances, lead to undesired cases as well. Electrical discharge in the SF₆ gas dielectric, caused by very fast overvoltages, spreads from the place of its occurrence towards all directions within the substation, which on discontinuities (e.g. connection bushings, cable bushings) also includes spreading onto the external side of the enclosure and earthed parts of the substation. Such overvoltages are characterized by a very high frequency for which even low inductances represent very high impedances. This paper is focused on simulation options of the transient connection GIS-overhead line in simulation software. Literature sources provide a fine description of the physical background of the observed phenomena. However, it is difficult to find a model presentation in certain software. Due to this fact, this paper shows possible ways of simulating the GIS-air connection with objects in ATP software.

Keywords – enclosure voltage, switching, transient overvoltages

1. INTRODUCTION

Gas Insulated Substations – GIS have been expressed in the recent decades, especially in urban, densely populated locations, where dimensional and safety advantages of gas insulated substations are particularly expressed. Low weight, compact design and simple maintenance are just a few advantages offered by SF₆ gas insulated substations. Maintenance and repair costs are lower compared to classic air insulated substations. Some of the advantages provided by modern gas insulated substations are:

- 50% lower fitting space requirements and lower weight,
- they can be fitted in climatically unsafe areas,
- prolonged maintenance intervals and expansion possibility.

An additional, very important advantage of gas insulated substations in comparison with the air insulated ones is safety. The safety of gas insulated substations is to be observed exclusively from the environmental protection aspect. In the closed pressure system design of the substation gas leaking is reduced to the standardized rate of 1% per year, while the other design (a hermetically closed system) does not require gas filling. The safety of people exposed to the substation, due to the fact that substations are located in inhabited areas, represents the second type of safety. Beside its unquestionable advantages, GIS also has its disadvantages. One of the main negative phenomena in gas insulated substations is the occurrence of very fast transients – VFT, whereat we differ between the so-called internal and external overvoltages [1]. External overvoltages refer to voltages between the enclosure and other parts of the substation (earth switch, earth, etc.), as well as to

voltages transferred to overhead lines and cables outside the substation.

Internal overvoltages refer to the voltages between the enclosed busbar towards other parts of the substation (earth switch, earth, enclosure, etc.). These overvoltages are caused by switching operations within GIS. One of the most frequent causes of overvoltages refers to switching operations of the disconnecter in the uncharged state. To exemplify this, the opening operation of the disconnecter with equivalent circuits for the capacitance circuit may be observed, Figure 1. This matches the opening operation of a part of the substation (e.g. single-line field) in the uncharged state, because it refers to the opening operation of low capacitance currents. While the disconnecter is closed, terminals on the source side and the load side (capacitance in Figure 1) are at the same potential. When the disconnecter contacts get disconnected during the opening, the terminal on the source side remains at the source potential. The terminal on the load side stays at the potential that matches the capacitor voltage at the moment of contacts being disconnected. So, the disconnecter terminal potential on the load side almost immediately changes its amount.

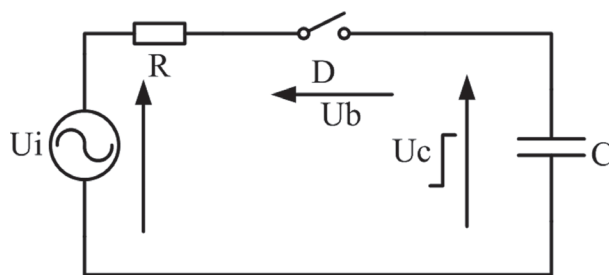


Fig. 1. Capacitive circuit opening (explanation of internal overvoltages generation)

This actually matches the immediate voltage change in the beginning of the substation's part being opened. As the change occurs very fast (almost immediate voltage increase/decrease), surge phenomena in the substation's part being opened appear, i.e. a current-voltage surge spreads through the substation's part being opened. Due to relatively slow movements of disconnecter contacts, dozens of such immediate potential (voltage) changes in the beginning of the substation's part being opened occur during a single switching operation [1]. Switching overvoltage phenomena and their occurrence manners are well described in literature [1, 2, 3, 4]. Measuring such phenomena is technically very demanding due to very fast occurrences and high voltages, so the accent in investigating these phenomena is placed on simulations in various software programs, whereat correct simulation of individual GIS elements is of great importance. With elements being properly simulated, the simulation results will match the real phenomena at a suitable level. In [1, 2, 3, 4, 5, 6, 7, 8, 9] a fine model presentation of individual GIS elements was provided for numerical simulations. Howev-

er, literature sources lack a detailed presentation of numerical values calculations of simulated GIS elements' parameters. Furthermore, no detailed ways of connecting the models in one of the simulation programs were provided. Due to these facts, this paper focuses on a more detailed presentation of model parameters calculation and ways of connecting in the ATP (Alternative Transient Program) software. For a more detailed simulation presentation, a GIS busbar with the transition to the overhead line and ground lead with a ground strap are observed here. This GIS part was chosen because several GIS elements (busbar, closed interrupter, closed disconnecter, ground lead), as well as connection lines and cables, are simulated as transmission lines with distributed parameters [1]. This detailed presentation of the GIS busbar simulation is provided in the case of observing external transient overvoltages. A part of GIS elements (open circuit breaker and disconnecter, transformer, earthing, ground lead) [1] are presented with concentrated parameters in which there are usually no doubts related to the use of an equivalent circuit. After this detailed presentation of the GIS busbar simulation, the second part of this paper presents the influence of certain parameters on external transient overvoltages.

This paper stresses the utilization of possibilities of the ATP-EMTP program for simulating these phenomena.

2. OCCURRENCE AND SPREADING OF A VOLTAGE SURGE ON THE GIS BUSBAR

Surge phenomena occur due to fast voltage changes on one end of the GIS busbar even with short busbar lengths (a few meters). The GIS busbar may therefore be simulated as a transmission line with distributed parameters. The voltage surge occurs due to a sudden potential change of one end of the GIS busbar as a result of the switching operation. As the busbar potential changes, the voltage between the busbar and the internal side of the GIS enclosure changes as well. The voltage surge occurring within the GIS enclosure spreads from the place of its occurrence through the busbar as the first line and the internal side of the enclosure as the second line. This is an incidence wave. At the termination point (connection bushing) from the GIS busbar onto the external connection line this surge transfers to the external side of the enclosure and the connected overhead line. A part of the incidence wave spreads along the external side of the enclosure as the first line and along the earth as the second line. This is the transient wave onto the external side of the enclosure. A part of the surge also spreads along the overhead line conductor as the first line and along the earth as the second line. This is the transient wave onto the connected overhead line. Thus, at the termination point from the gas insulated substation onto the overhead line reflection, transfer and other surge phenomena occur. These surge phenomena occur because the three lines (busbar-internal side of the enclosure, external side of the enclosure-earth and overhead line-earth)

have different surge impedances and surge propagation velocities. This description of surge phenomena is shown in Figure 2.

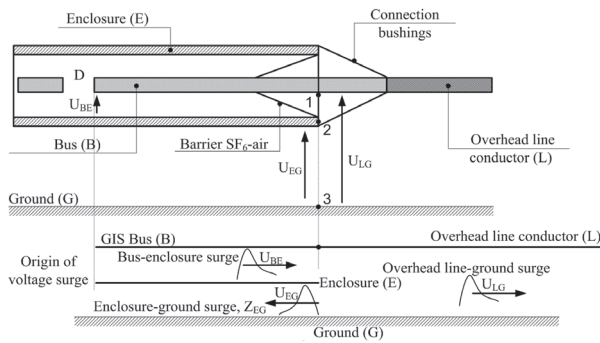


Fig.2. Voltage surges on a GIS-overhead line connection

2.1. Transient enclosure voltage

As the surge spreads along the line consisting of the external enclosure and earth and due to the earthing resistance, the external side of the enclosure reaches a certain potential according to the reference point (earth) with zero potential. Thus, on the GIS busbar enclosure voltage towards earth occurs. This happens due to the change velocity of the voltage that caused voltage surge propagation. As this phenomenon occurs very fast, frequencies of induced voltages will be measured in MHz. The literature states frequencies in the amount of 100 kHz – 50 MHz [1]. At these frequencies, the earthing impedance (especially the inductive component) reaches high values and the enclosure acts as if being non-earthed although it is earthed. This applies to short overvoltage duration. After the transient phenomenon is completed, the enclosure reaches the earth potential because it is earthed.

3. MODELING CERTAIN GIS PARTS

3.1. Enclosed busbar, transfer GIS-overhead line and overhead line

Figure 3 shows the sectional view of the GIS busbar and connection to the overhead line, as well as the equivalent circuit with transmission lines.

As mentioned earlier, due to fast voltage changes electromagnetic surges occur during switching operations. Due to accentuated surge phenomena, in calculations the substation is modeled with distributed parameters transmission lines. [1] states that these transmission lines may be modeled as lossless lines. In Figure 2, it can be noticed that there are three transmission lines: busbar-to-enclosure line, enclosure-to-earth line and overhead conductor-to-earth line. At the moment of a disruptive discharge or an interruption between the disconnect D contacts (Figure 3), a voltage surge between the busbar and the enclosure forms.

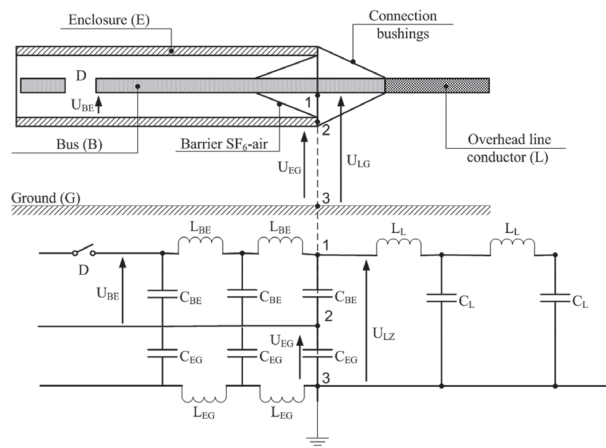


Fig.3. Connection of the GIS-overhead line and equivalent with transmission lines

This surge travels between the busbar and the enclosure towards the overhead line. Spreading of this surge is determined by L_{BE} (unit inductance) and C_{BE} (unit capacitance) parameters defined by mutual geometry of the busbar and the enclosure. At the GIS-to-overhead line junction point, this incidence surge is reflected and refracted. A part of the surge passes onto the overhead line and continues to spread along the overhead line. Spreading of this surge is determined by unit inductance (L_L) and capacitance (C_L) of the line that depend on the geometry and the position of the conductor with regard to earth. The other part of incidence surge, at the GIS-to-overhead line junction point, passes onto the external side of the enclosure and continues to spread between the enclosure and earth. The way in which this surge acts is determined by L_{EG} and C_{EG} parameters that depend on the geometry and position of the enclosure with regard to earth.

Based on such physical description of surge phenomena, a model was made in the ATPDraw 5.5 program. In ATP, there are several blocks by means of which the overhead line may be modeled. These blocks are: distributed transposed lines and untransposed lines and LCC (Line and Cable Constants). In this paper, the case shown in Figure 3 was modeled in two ways, i.e. by means of distributed lines blocks and LCC blocks.

3.2. Ground leads and straps

[1, 2, 8] refer to two ways of modeling ground lead and strap. The first way is modeling with concentrated parameters and the second one is modeling with lines with distributed parameters, whereat it is stated that the way of modeling the earth line affects the results more significantly than the way of modeling the earthing. At high frequencies the earthing takes on high impedance, so only a small part of the earthing, closest to the surge entrance point, takes part in the voltage/current surge diversion. For ground lead modeling, although shorter, models with distributed parameters are recommended due to high frequencies, whereat

the specific nature of ground lead, which refers to its position with regard to earth, is stressed. Ground lead usually goes from the enclosure towards the earthing perpendicularly to earth. Due to this fact, ground lead is a line with distributed parameters that vary in each point, depending on the point height on the ground lead. Thus, the surge travelling along ground lead actually encounters constant variations in surge impedance along ground lead. [1, 2] state that the surge impedance of a vertical ground lead is calculated by means of the following formula:

$$Z_c = 60 \cdot \ln\left(\frac{2 \cdot \sqrt{2} \cdot h}{r}\right) \quad (1)$$

whereby h refers to the average height above earth of the vertical ground lead and r refers to the ground lead radius (earthing strap or round conductor radius). In [1], the recommendation for sectioning the ground lead into several parts was given. After ground lead is divided into several parts, each part is modeled by a line with distributed parameters. Surge impedance of each part is calculated according to expression (1) with the average above-earth height of each section.

4. MODELING IN ATPDraw 5.5.

Based on the aforementioned considerations and Figure 3, lines with distributed parameters that are to be modeled in ATP may be presented as shown in Figure 4.

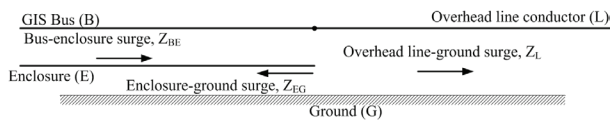


Fig.4. : Surge phenomena at the GIS-overhead conductor junction

From Figure 4 it is visible that the busbar and enclosure-to-earth voltages and the in-between voltages shall be determined by the propagation of two surges: busbar-to-enclosure surge and enclosure-to-earth surge.

4.1. Frequency, time step, calculation time

[1] states the following expression for the response frequency (in MHz) of the lossless distributed parameter line, whereby the propagation velocity is close to that of light:

$$f = \frac{75}{l} \quad (2)$$

where l refers to the duct length. Unit resistance and unit inductance significantly depend on the frequency, whereby they are calculated in the same way as inductive and capacitive resistances. Thus, while modeling, it

is important to select the frequency at which line parameters are calculated. Here the calculation frequency is selected according to (2). The expression for the propagation velocity follows [1] from (2):

$$\tau = \frac{1}{4 \cdot f} \quad (3)$$

According to [1], the time step in ATP must be equal to or less than one-half the shortest transit time. Thus, the time step of the simulation is defined by:

$$\Delta T \leq \frac{\tau_{\min}}{2} \quad (4)$$

According to [1], the duration of the observed transient phenomena is in the range of a few hundred nanoseconds. Here the selected simulation interval equals $1\mu\text{s}$.

4.2. Instantaneous change in voltage

The ATP database contains a Source Ramp block. One of its terminals is earthed. For modeling an instantaneous voltage phenomenon between the busbar and the enclosure, the ideal 1:1 transmission ratio of the transformer was used. The Source Ramp block was connected to the transformer primary, and the beginning of the distributed parameter line between the busbar and the enclosure to the secondary. The resistor in series with the source has very small values ($1\text{E-}6\Omega$) and does not affect the results. It was selected due to the ATP operating conditions (without it, the program reports an error).

4.3. Busbar-to-enclosure transmission line and enclosure-to-earth transmission line

For this and all other transmission lines two models were made: modeling the transmission line with the LCC block (model A) and modeling the transmission line with the Distributed parameter line block (model B). Model A modeling (with the LCC block) was made by selecting the "Enclosing Pipe in Air" option along with the Bergeron line model. At creating the LCC model, the program, with such settings, calculates and shows unit line parameters ($Z1$ and $Y1$ matrix), surge impedance (Z_c), propagation velocity on the line and transformation matrices and modal parameters in multi-phase lines. By means of the LCC block the busbar-to-enclosure line and the enclosure-to-earth line were modeled here as one line and the other line. Regarding the enclosure-to-busbar line, data on dimensions of the busbar and the enclosure, as well as the height above earth of the enclosure were entered. Regarding the enclosure-to-earth line, data on the enclosure dimensions and the height above earth of the enclosure were entered. Both of these lines were modeled as a single-phase line, the busbar-to-enclosure line not being earthed. Such modeling with two single-phase lines can be explained by

a detailed observation of the calculation manner and the way the ATP blocks were applied. If in ATP the LCC block is used for modeling the pipe conductor as a two-phase line with the Bergeron model, the calculation result shows the following one. Modal surge impedances and modal propagation velocities of this two-phase line equal surge impedances and propagation velocities for two single-phase lines, i.e. a single modal surge impedance and propagation velocity equal the surge impedance and propagation velocity for a single pipe conductor. The second modal surge impedance and propagation velocity equal the surge impedance and propagation velocity for a line modeled in a pipe above earth. As the modal analysis calculates voltage surges in each mode for a single mode independent of the other, it is to be concluded that modal voltage surges spread independently of one another. This matches a single surge travelling throughout the line with a single pipe conductor, while the other surge travels throughout the pipe above earth. Regarding model B (with the Distributed parameter line block), data on modal components were entered, which refer to modal unit resistances, modal surge impedances and modal propagation velocities. These data were not calculated "manually", but were taken from calculations obtained by means of LCC objects. References [2, 6, 3 and 4] provide expressions for calculating unit capacitances and inductances of the enclosed GIS busbar. However, the advantage of calculating these parameters in ATP was used here. In model B, the busbar-to-enclosure line was modeled as a two-phase line with the busbar as one and the enclosure as the other phase. Parameters for the two-phase line in the model B may be obtained by calculating surge impedances and propagation velocities for two single-phase lines from model A or by calculating modal surge impedances and propagation ve-

locities for a two-phase line. However, if the two-phase line from model B is modeled with the LCC block as a two-phase line, the pipe conductor will not deliver the expected result (enclosure potential equals zero). This is so due to the fact that in the pipe conductor model ATP does not model the pipe as the second phase conductor, although the two-phase block option is on. This also applies to modeling a two-phase line as a single core cable. It is also not possible to use any available line model in ATP for modeling a two-phase line consisting of two concentric conductors.

4.4. Overhead transmission line

For model A in the LCC block Overhead line was selected and the line geometry and height above ground was entered along with selecting the Bergeron line model. Block parameters (unit and surge impedance, propagation velocity) in model B were taken from the Bergeron model calculation of the LCC block. In both cases the overhead line was modeled as a single-phase line. For the voltage transfer between the busbar and the enclosure, an ideal transformer with the 1:1 transmission ratio was used at the beginning of the overhead line.

4.5. Transmission ground lead line

As the LCC block does not provide the possibility of setting up a vertical line, for model A, as well as for model B, ground lead was modeled by means of the Distributed parameter line block, where it was used as a lossless line with surge impedance according to [1]. The propagation velocity amounted to 96% of the light velocity ($v = 0,96 \cdot c$), as recommended by [1]. This line was connected to the end of the enclosure-to-earth line.

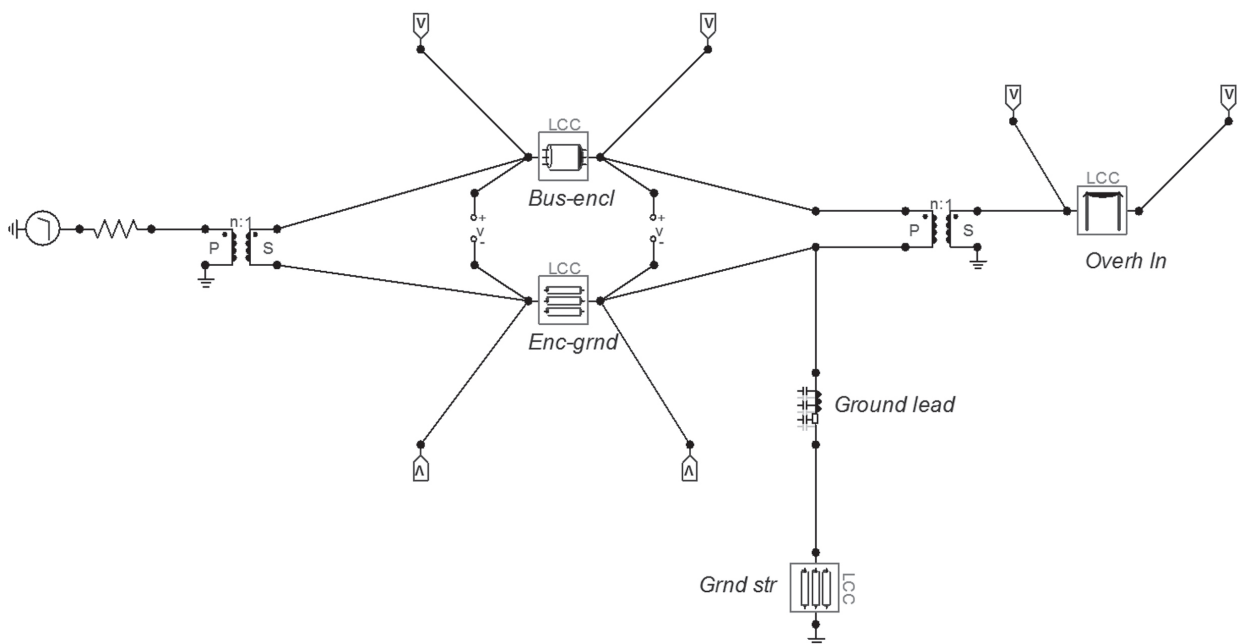


Fig.5. ATP diagram for model A (with LCC blocks)

4.6. Earthing transmission line

In model A, the earthing was modeled by means of the LCC block as a single core cable without a sheath and display, in the ground. Also, the Bergeron line model was used as a single-phase line. In model B, the earthing was modeled by means of the Distributed parameter line block, with parameters' values being taken from LCC model calculations.

4.7. ATPDraw 5.5. diagram

Based on the facts described in parts 4.2.-4.6., Figures 5 (for model A) and 6 (for model B) show an ATP model of a simple GIS case from Figure 2. In model A, the busbar-to-enclosure transmission line is modeled by means of two single-phase lines, whereas model B is modeled with one two-phase line.

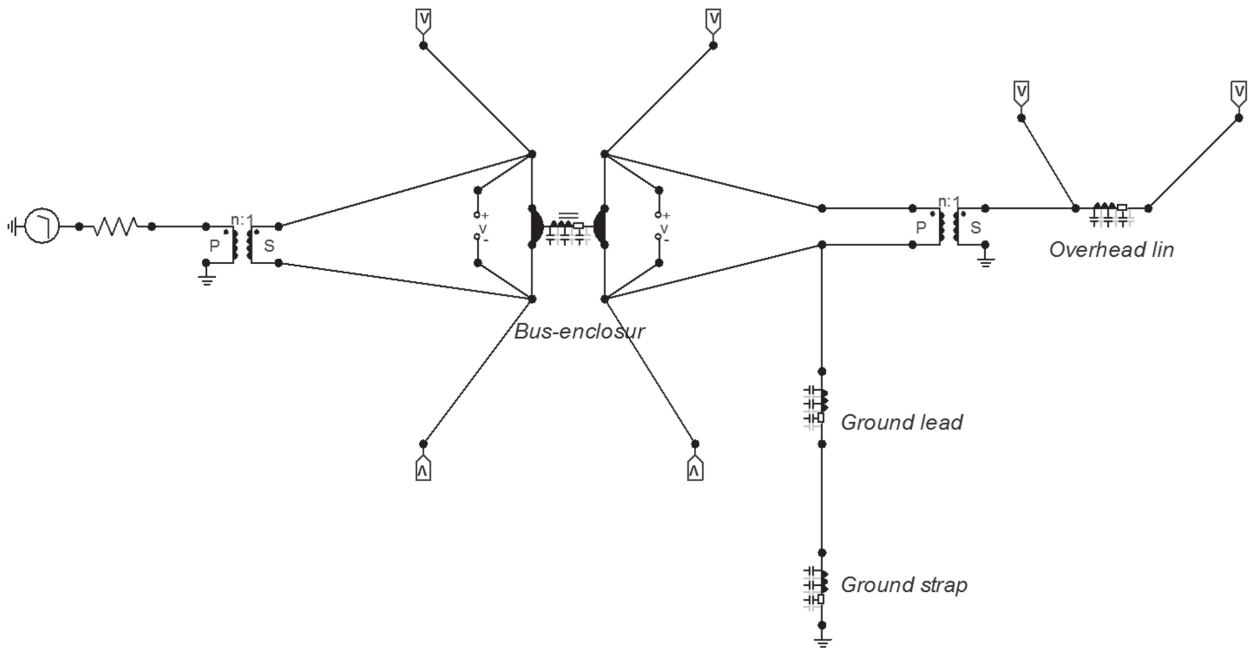


Fig.6. ATP diagram for model B (with Distributed untransposed parameter line blocks)

5. SIMULATION RESULTS AND RESULT ANALYSIS

Simulations were carried out for the case related to low voltage tests [1] with the source voltage increase amounting to 100 V in the period of 4 ns and the source resistance amounting to 75 Ω . Regarding the data shown in Table 1, model A (Figure 5) and model B (Fig-

ure 6) simulations were carried out. A part of waveforms obtained through simulations is shown in Figures 7-21. Figures 7-16 show a comparative presentation of the same voltages obtained by means of both models.

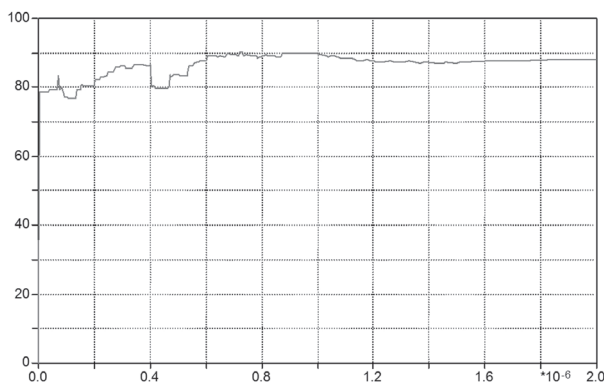


Fig.7. Voltage between the busbar and the enclosure at the beginning of the busbar-to-enclosure line (model A)

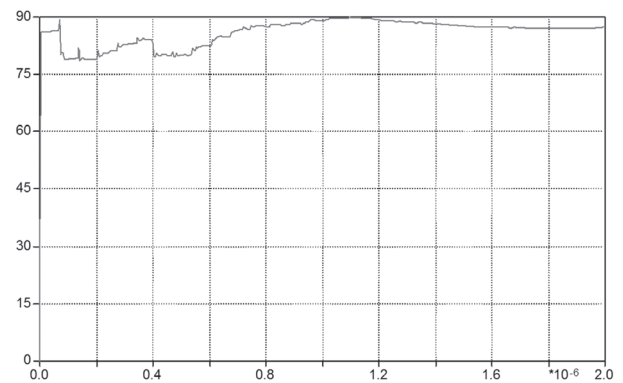


Fig.8. Voltage between the busbar and the enclosure at the beginning of the busbar-to-enclosure line (model B)

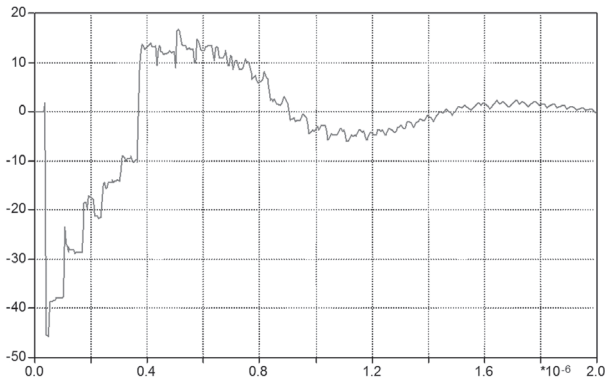


Fig.9. Enclosure voltage towards earth at the GIS-to-overhead line junction point (model A)

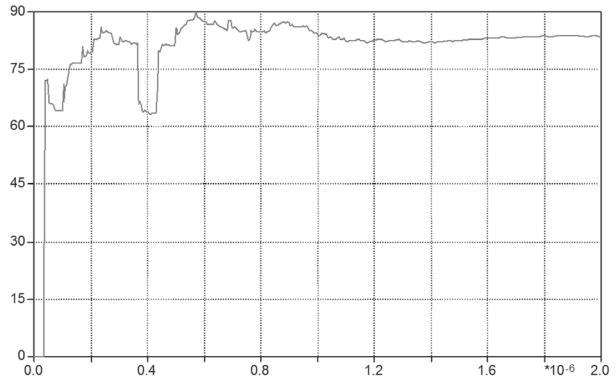


Fig.10. Voltage between the busbar and the enclosure at the Enclosure voltage towards earth at the GIS-to-overhead line junction point (model A)

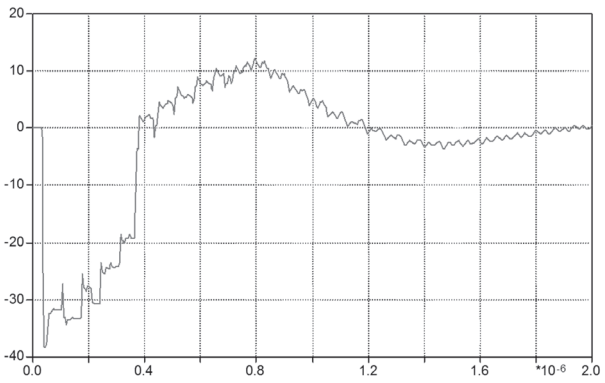


Fig.11. Enclosure voltage towards earth at the GIS-to-overhead line junction point (model B)

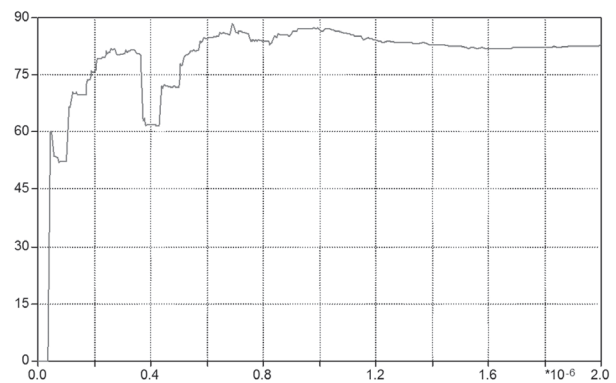


Fig.12. Voltage between the busbar and the enclosure at the Enclosure voltage towards earth at the GIS-to-overhead line junction point (model B)

Figures 7-12 were obtained for the basic data provided in Table 1.

Table 1. Basic input data for the simulation and results for the transmission line models

GIS busbar	Internal busbar radius	$R_{SU} [m]$	0.0383	
	External busbar radius	$R_{SV} [m]$	0.051	
	Internal enclosure radius	$R_{OU} [m]$	0.1459	
	External enclosure radius	$R_{OV} [m]$	0.1535	
	Busbar length	$l_s [m]$	10	
	Specific resistance of the busbar	$\rho_s [\Omega m]$	$1.543 \cdot 10^{-8}$	
	Specific resistance of the enclosure	$\rho_o [\Omega m]$	$2.65 \cdot 10^{-8}$	
Overhead line	Height above earth	$H [m]$	2	
	Conductor radius	$R_{NV} [m]$	0.01	
	Height of the tower top	$H_v [m]$	15	
	Heights in the middle of the midspan sag	$H_{VM} [m]$	10	
	Length	$l_{NV} [km]$	5	
Earth	DC unit resistance of the conductor	$R_v [\Omega/km]$	0.2374	
	Specific earth resistance	$\rho_e [\Omega m]$	100	
Ground lead	Length	$l_{zv} [m]$	2	
	Strap width	$d_{zv} [m]$	0.04	
Ground strap	Length	$l_{uz} [m]$	25	
	External diameter	$R_{UZ} [m]$	0.04	
	Specific resistance	$\rho_{uz} [\Omega m]$	$2.65 \cdot 10^{-8}$	
MODELS OF DISTRIBUTED PARAMETERS TRANSMISSION LINES (calculation results in ATP for the Bergeron line model)	Busbar-to-enclosure	Frequency for the parameter calculation	$f_{SO} [Hz]$	$7.5 \cdot 10^6$
		Surge impedance	$Z_{SO} [\Omega]$	63.032
		Propagation velocity	$v_{SO} [m/s]$	$2.9975 \cdot 10^8$
	Enclosure-to-earth	Surge impedance	$Z_{OZ} [\Omega]$	207.987
		Propagation velocity	$v_{OZ} [m/s]$	$2.8177 \cdot 10^8$
	Overhead line conductor-to-earth	Frequency for the parameter calculation	$f_{NV} [Hz]$	15 000
		Surge impedance	$Z_{NV} [\Omega]$	571.48
		Propagation velocity	$v_{NV} [m/s]$	$2.4393 \cdot 10^8$
	Earthing	Frequency for the parameter calculation	$f_{UZ} [Hz]$	$3 \cdot 10^6$
		Surge impedance	$Z_{UZ} [\Omega]$	152.53
		Propagation velocity	$v_{UZ} [m/s]$	$1.5848 \cdot 10^8$
	Ground lead	Surge impedance	$Z_{UZ} [\Omega]$	255
Propagation velocity		$v_{UZ} [m/s]$	3·108	

As literature sources state that, due to high frequencies, lossless lines may be used, these neglecting effects are investigated in this paper as well. Figures 13 and 14 show enclosure-to-earth voltages at the GIS-to-overhead line junction point when line losses are neglected, for both ATP models. Figures 15 and 16 show busbar-to-earth voltages at the beginning of the busbar-to-enclosure line for modeling lossless lines. In model A, the lossless line is modeled by setting the

earth resistance to zero and the specific values of busbars, pipes and the overhead line to a very low value (value range amounting to 10^{-18}). In model B, the lossless lines are modeled by setting the model's operating resistance to zero. In model B, the propagation velocities from the previous LCC block calculation are kept. These simulations were carried out with the simulation duration amounting to 5 μ s.

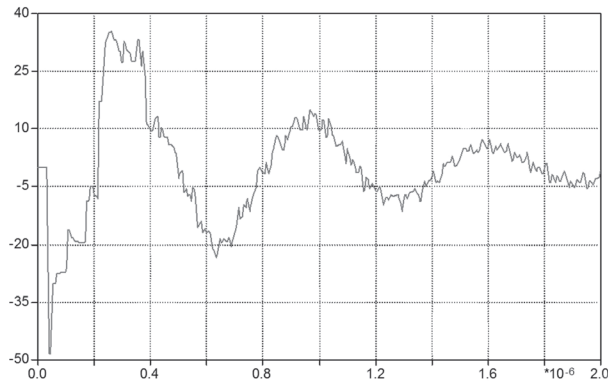


Fig.13. Enclosure-to-earth voltage at the GIS-to-overhead line junction point (model A), lossless

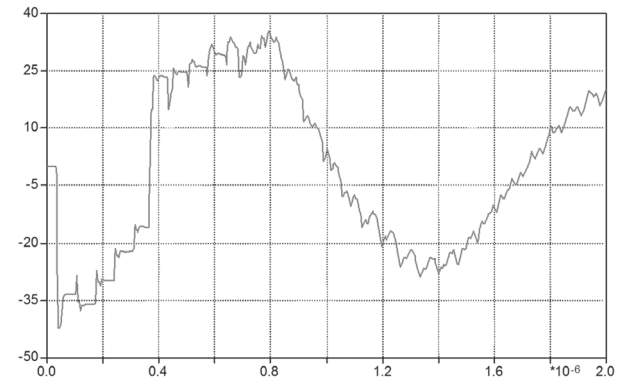


Fig.14. Enclosure-to-earth voltage at the GIS-to-overhead line junction point (model B), lossless

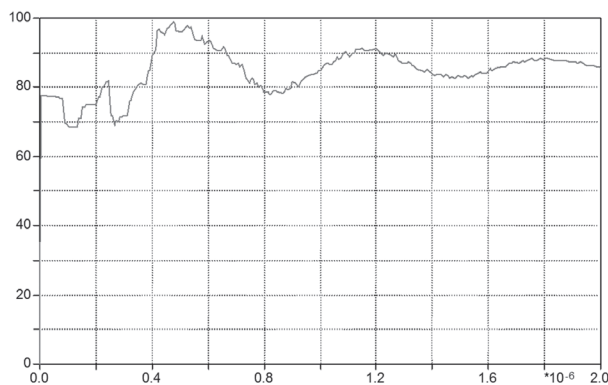


Fig.15. Voltage between the busbar and the enclosure at the beginning of the busbar-to-enclosure line (model A), lossless

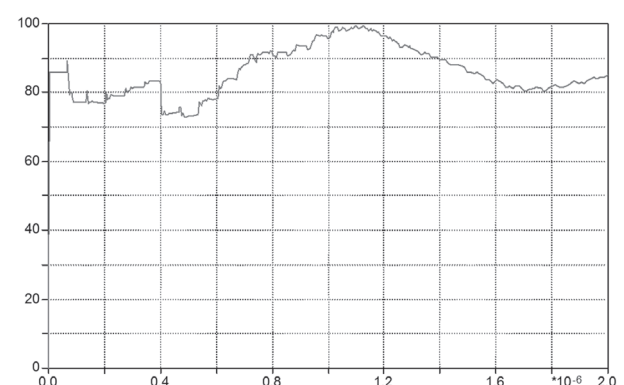


Fig.16. Voltage between the busbar and the enclosure at the beginning of the busbar-to-enclosure line (model B), lossless

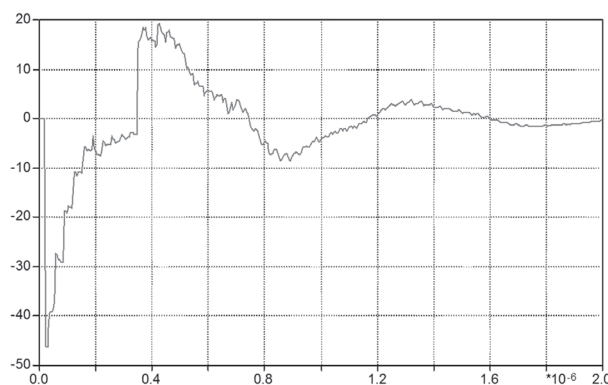


Fig.17. Enclosure-to-earth voltage at the GIS-to-overhead line junction point (model A), 5 m GIS

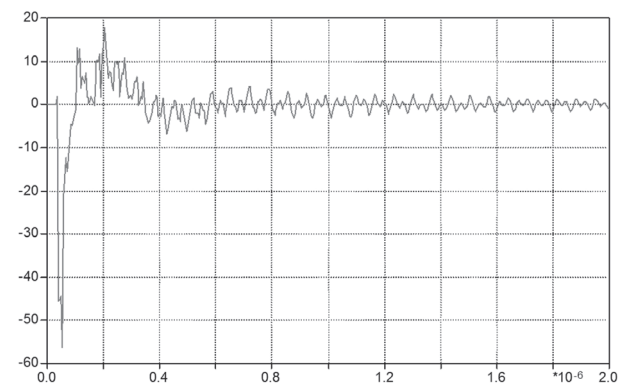


Fig.18. Enclosure-to-earth voltage at the GIS-to-overhead line junction point (model A), RL earthing

Furthermore, Figure 17 shows the enclosure-to-earth voltage at the GIS-to-overhead line junction point for the GIS busbar being two times shorter and all other parameters remaining the same as in Figure 7, model A. Figure 18 shows the same voltage for modeling the earthing with concentrated R and L parameters with all other parameters equal to the initial ones, for model A.

Figure 19 shows the enclosure-to-earth voltage at the GIS-to-overhead line junction point for a three

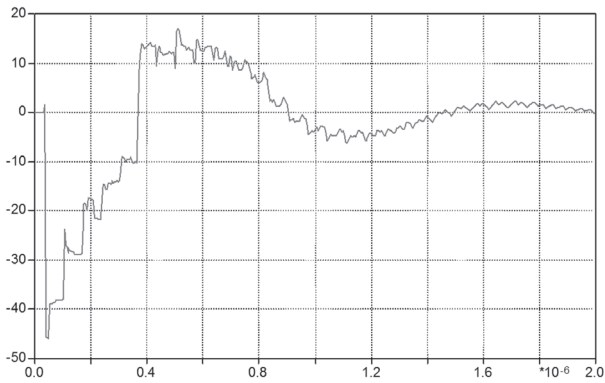


Fig.19. Enclosure-to-earth voltage at the GIS-to-overhead line junction point (model A), 15 km overhead line

times longer overhead line, and Figure 20 for ten times shorter overhead line than the initially observed one, for model A. Figure 21 shows this voltage for the case involving sectioning the earth line with regard to height into four equal parts. Figure 22 shows the voltage between the enclosure points at the beginning and at the end of the busbar-to-enclosure line - both figures are simulated by means of model A.

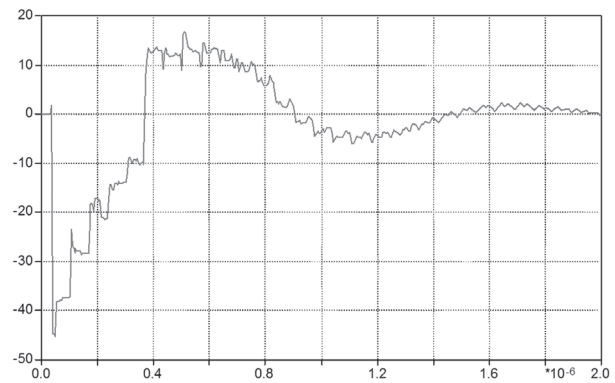


Fig.20. Enclosure-to-earth voltage at the GIS-to-overhead line junction point (model A), 0.5 km overhead line

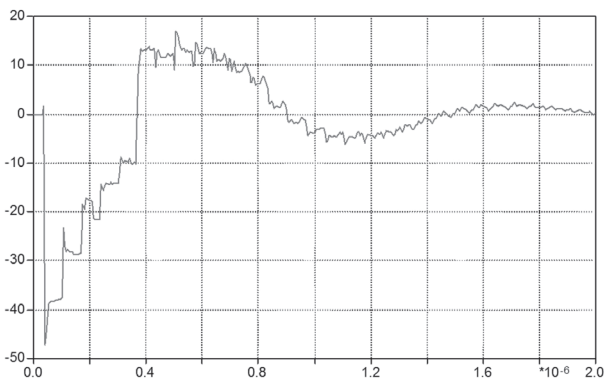


Fig.21. Enclosure-to-earth voltage at the GIS-to-overhead line junction point (model A), sectioned ground lead

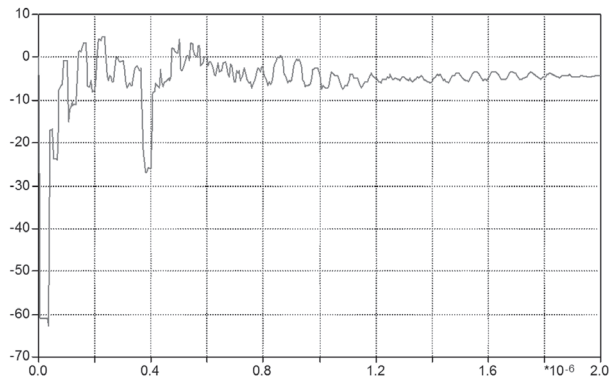


Fig.22. Voltage between different points along the enclosure (model A), sectioned ground lead

By comparing the matching waveforms in Figures 7-11, insignificant differences between models A and B may be noticed. The most significant difference refers to the momentary values of the enclosure voltage (Figures 9 and 10). Model A provides somewhat higher values of the enclosure-to-earth voltage. The difference between models is more expressed in the case related to modeling with lossless lines. Both models result in the enclosure voltage that lasts longer and has larger oscillations if compared to modeling with lines with losses. Also, model B in this case provides a somewhat longer duration and larger voltage oscillations than model A (Figures 13 and 14). These expressed oscillations may be explained by the fact that operating resistances that attenuate such oscillations are missing. The

highest values of the enclosure voltage remain close to the values for modeling with lines with losses. Generally, if losses are neglected, the transient phenomenon obtained by simulation is prolonged. By comparing Figures 9 and 17 it may be concluded that the busbar length has insignificant effects on the highest values of the enclosure voltage. This conclusion is to be carefully considered, because the enclosure voltage is significantly influenced by the GIS configuration. Modeling the earthing with concentrated parameters shortens the enclosure voltage duration, whereby the highest value is somewhat higher, as noticeable from the comparison of Figures 9 and 18. In modeling concentrated parameters earthing oscillations are more expressed, but their amplitudes are smaller. From Figures 9, 19

and 20 it is visible that the length of the connected overhead line does not affect the enclosure voltage. By comparing Figures 9 and 21 it can also be concluded that sectioning the ground lead into several transmission lines in this case has no effect on the enclosure voltage. This probably results from a shorter ground lead length and a very simple GIS example. Figure 21 illustrates that there is a potential difference, i.e. voltage, along the enclosure itself. This results from the fact that the observed phenomenon is a waveform one. Due to the final propagation velocity, different points along the enclosure will also have different potentials at the same moment.

By comparing increasing source voltage values with the highest enclosure-to-earth voltage values, it can be concluded that the enclosure voltage amounts to 40-50% of the source voltage, in the case of a simple GIS structure in question.

The obtained waveforms are of similar shape, as in [1]. Therefore, the proposed models can be used for observation of internal overvoltages in the case of a simple GIS busbar. Additional comparisons of simulated results and measurement data are needed to confirm a general application of the proposed model.

6. CONCLUSION

The basic purpose of this paper refers to an additional clarification of modeling a simple GIS busbar in the ATPDraw simulation program. Two ways of modeling with program blocks are presented. One way refers to modeling the busbar-to-enclosure transmission line by means of two single-phase lines. The other way is modeling by means of a single two-phase line. These models were developed by observing physical phenomena during a sudden busbar potential change caused by switching operations. The biggest problem with developing these models refers to the selection and the way of connecting the blocks in ATP. A simple case of transferring the GIS busbar to an overhead line was taken into consideration, as there were many uncertainties with modeling this transfer. This results from the fact that the literature dealing with such phenomena are mostly concerned with physical-mathematical modeling of individual GIS parts. However, it is very difficult to find a model portrayed in a certain program in any of them. This fact makes the exploration of such phenomena very difficult. Additional tests, simulations and comparisons with measured data are needed for models evaluation. The main purpose of this paper is to give details of a model of a simple GIS busbar that are not visible in most of the literature.

Due to its complexity (waveform phenomena), GIS modeling for observing specific phenomena is extremely complex. By analyzing simulation results, it can be concluded that such models and simulations allow a more detailed insight into an observed phenomenon.

By means of such simulation models it is possible to investigate the influence of individual phenomena on the potential rise of the GIS enclosure. Based on the results of such simulations, further measures for decreasing the potential rise of the GIS enclosure may be suggested. For further investigations of these phenomena, more simulations in programs dealing with electromagnetic fields are to be deployed.

ACKNOWLEDGEMENTS

The authors wish to thank Ivana Jurković, BA, for translating this paper into English.

7. REFERENCES

- [1] J.A. Martinez, P. Chowdhuri, R. Iravani, A. Keri, D. Povh, Modeling Guidelines for Very Fast Transients in Gas Isolated Substations, IEEE PES Special Publication Modeling and Analysis of System Transients, 1998. Online available: <http://www.ee.umanitoba.ca/~gole/wg15.08.09/vfast.pdf> (20 August 2011)
- [2] T. Honma (editor), Advanced Computational Electromagnetics, Selected Papers of the 3rd Japan-Hungary Joint Seminar on Applied Electromagnetics in Materials and Computation, IOS Press, Amsterdam 1995.
- [3] J.V.G. Rama Rao, J. Amarnath, S. Kamakshiah, Simulation and Measurement of Very Fast Transient over Voltages in a 245 kV GIS and Research on Suppressing Method Using Ferrite Rings, ARPN Journal of Engineering and Applied Sciences, pp. 88-95, Vol.5, No. 5, May 2010.
- [4] M. Kondalu, G.S. Reddy, P.S. Subramanyam, Estimation of Transient over Voltages in Gas Insulated busduct from 220 kV Gas Insulated Substation, International Journal of Computer Applications, pp. 1-5, Vol. 20, No. 8, April 2011 .
- [5] C.Y. Lui, Computational study of very fast transients in GIS with special reference to effects of trapped charge and risetime on overvoltage amplitude, IEEE Proc.-Gener. Transm.Distrib., pp. 485-490, Vol. 141, No. 5, September 1994 .
- [6] S. Bojić, I.Uglešić, Researching the Efficiency of Measures for Decreasing the Transient Enclosure Voltage Rise of the Gas Insulated Switchgears, Online available on: <http://www.ipst.org/TechPapers/2001/IPST01Paper090.pdf> (20 September 2011)

- [7] Ž. Štih, S. Banić, K. Meštrović, S. Berberović, Elektromagnetska kompatibilnost u oklopljenom SF6 postrojenju TS 220/110/35/20(10) kV Plat (Electromagnetic Compatibility in Gas-insulated Substation TS 220/110/35/20(10) kV PLAT), 9. Savjetovanje HRO CIGRE, Cavtat, studeni 2009. Online available on: http://bib.irb.hr/datoteka/392134.EMC_u_TS_Plat_v3.pdf (18 September 2011)
- [8] S. Hutter, I. Uglešić, S. Bojić, Modeliranje trolno oklopljenih plinom SF6 izoliranih VN postrojenja za proračune vrlo brzih prijelaznih prenapona (Modeling of the Three Phase Encapsulated Gas SF6 Insulated HV Switchgear for the Calculation of Very Fast Transient Overvoltages), 6. Savjetovanje HK CIGRE, Cavtat, studeni 2003. Online available on: <http://bib.irb.hr/prikazi-rad?rad=147039> (20 September 2011)
- [9] I. Uglešić, S. Hutter, V. Milardić, I. Ivanković, B. Filipović-Grčić, Electromagnetic Disturbances of the Secondary Circuits in Gas Insulated Substation due to Disconnecter Switching, International Conference on Power Systems Transients - IPST 2003 in New Orleans, USA, September 28th - November 2nd, 2003 . Online available on: <http://www.ipst.org/TechPapers/2003/IPST03Paper14a-2.pdf> (02 September 2011)